Molecular Cell
Article

Frameshift Mutagenesis and Microsatellite Instability Induced by Human Alkyladenine DNA Glycosylase

Joanna Klapacz,[1,3] Gondichatnahalli M. Lingaraju,[1,3] Haiwei H. Guo,[2,3] Dharini Shah,[1] Ayelet Moar-Shoshani,[1] Lawrence A. Loeb,[2] and Leona D. Samson[1,*]
[1]Departments of Biological Engineering and Biology and Center for Environmental Health Sciences, Massachusetts Institute of Technology, 77 Massachusetts Avenue, Cambridge, MA 02139, USA
[2]Department of Pathology, The Joseph Gottstein Memorial Cancer Research Laboratory, University of Washington, Seattle, WA 98195, USA
[3]These authors contributed equally to this work
*Correspondence: lsamson@mit.edu
DOI 10.1016/j.molcel.2010.01.038

SUMMARY

Human alkyladenine DNA glycosylase (hAAG) excises alkylated purines, hypoxanthine, and etheno bases from DNA to form abasic (AP) sites. Surprisingly, elevated expression of hAAG increases spontaneous frameshift mutagenesis. By random mutagenesis of eight active site residues, we isolated hAAG-Y127I/H136L double mutant that induces even higher rates of frameshift mutation than does the wild-type hAAG; the Y127I mutation accounts for the majority of the hAAG-Y127I/H136L-induced mutator phenotype. The hAAG-Y127I/H136L and hAAG-Y127I mutants increased the rate of spontaneous frameshifts by up to 120-fold in *S. cerevisiae* and also induced high rates of microsatellite instability (MSI) in human cells. hAAG and its mutants bind DNA containing one and two base-pair loops with significant affinity, thus shielding them from mismatch repair; the strength of such binding correlates with their ability to induce the mutator phenotype. This study provides important insights into the mechanism of hAAG-induced genomic instability.

INTRODUCTION

DNA continuously suffers damage as a consequence of normal cellular metabolism and as a result of attack by environmental agents (Friedberg, 2006; Lindahl, 1993). Base excision repair (BER) is the major pathway that defends cells against DNA base damage such as alkylation, oxidation, and deamination (Fan and Wilson, 2005), and BER is initiated by one of a collection of DNA glycosylases, each of which excises specific modified bases leaving abasic (AP) sites in the DNA backbone. AP endonuclease or AP lyase activities nick DNA at the AP site, and the 5′ and 3′ ends are processed such that DNA polymerase can fill the gap and the DNA ends can be ligated to complete the repair process.

A variety of modified DNA bases are recognized and processed by the so-called 3-methyladenine (3MeA) DNA glycosylases, including positively charged N3- and N7-alkylated purines, deaminated adenine (hypoxanthine, Hx) and guanine (xanthine, X), and cyclic etheno adducts of adenine (1,N^6-ethenoadenine, εA) and guanine (3,N^2-ethenoguanine, εG) induced under conditions of lipid peroxidation (O'Brien and Ellenberger, 2004a, 2004b). These enzymes exhibit significant differences in their ability to excise lesions within polynucleotide repeats (Lingaraju et al., 2008; Wyatt and Samson, 2000) and can also excise normal, undamaged purines from DNA, albeit with very low efficiency (Berdal et al., 1998; Wyatt et al., 1999). The crystal structures of 3MeA DNA glycosylases from *E. coli* (AlkA and Tag) and from humans (hAAG, also called MPG or ANPG) reveal that these enzymes position the flipped out damaged base in the electron-rich, aromatic active site (Drohat et al., 2002; Hollis et al., 2000; Lau et al., 1998). When hAAG is complexed with an oligo containing the εA substrate, εA snugly stacks between Tyr127 on one side and His136 plus Tyr159 on the other (Lau et al., 2000) (Figure 1A). This triplet of residues captures and stabilizes the base in the active site through π-stacking interactions and a hydrogen bond donated from the main-chain amide of His136 to the N6 of εA (Lau et al., 2000).

We have proposed that, under certain circumstances, increased, rather than decreased, levels of DNA glycosylase can lead to elevated spontaneous mutation and genomic instability (Glassner et al., 1998a, 1998b; Guo and Loeb, 2003; Hofseth et al., 2003; Posnick and Samson, 1999; Xiao and Samson, 1993). We showed that higher than normal levels of *S. cerevisiae* 3MeA DNA glycosylase (Mag1) induce elevated rates of both base-pair substitutions and frameshift mutations in yeast (Glassner et al., 1998b; Hofseth et al., 2003; Rusyn et al., 2007). Ulcerative colitis (UC), a chronic inflammatory condition of the large intestine, is frequently associated with microsatellite instability (MSI) and exhibits a 19-fold increased risk of developing colorectal cancer (Gillen et al., 1994). We reported that chronic inflammation associated with UC is accompanied by an increase in hAAG levels and activity in the inflamed tissues (Hofseth et al., 2003) and positively correlated with increased MSI compared to uninflamed epithelia of UC patients. Indeed, increasing hAAG levels in cultured human cells induced an MSI phenotype and increased spontaneous frameshift mutation rates in yeast cells (Hofseth et al., 2003). We inferred that inappropriate expression of yeast and human 3MeA DNA glycosylases can increase the accumulation of BER intermediates and that these BER intermediates promote genomic instability.

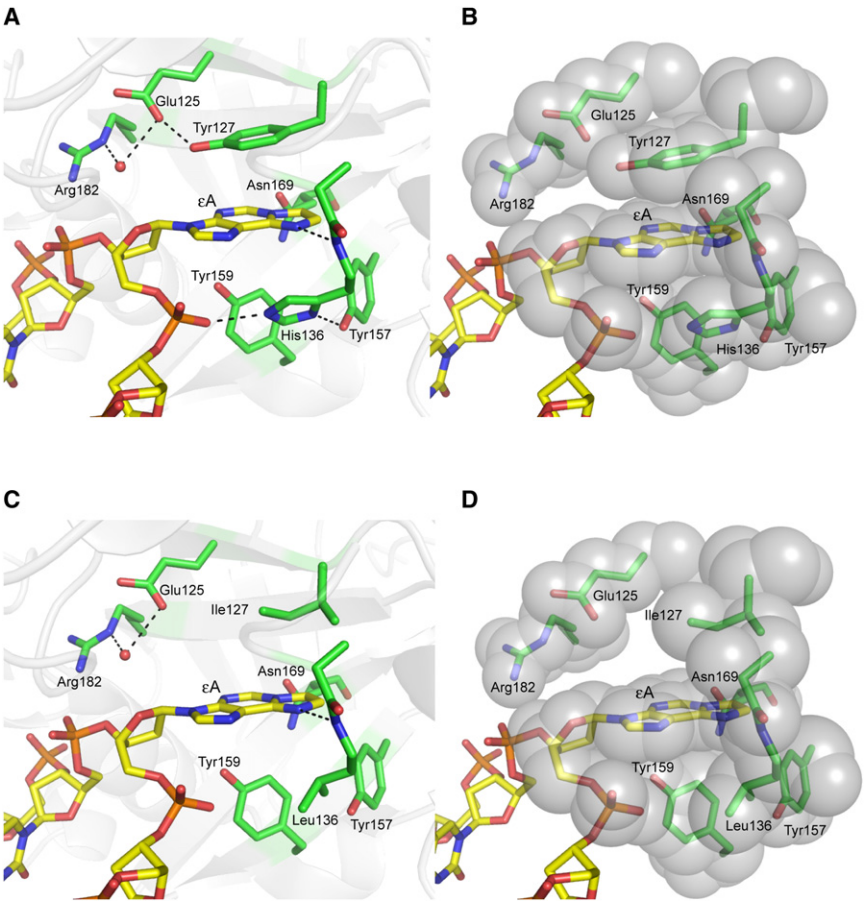

Figure 1. Active Site Residues of hAAG Interacting with εA

(A–D) The amino acid side chains are colored green, εA containing DNA in yellow, and a nucleophilic water molecule as a sphere in red. Architecture of hAAG's active site showing the residues that interact with εA (PDB ID 1f4r) (A) as ribbon model and (B) as space-filling model (Lau et al., 2000). The mutations of Y127I and H136L modeled into the active site of hAAG (PDB ID 1f4r) as (C) ribbon model and (D) space-filling model.

In this study, we explore the mechanism by which hAAG induces genomic instability. We isolated hAAG mutants that induce even stronger mutator phenotypes in *E. coli*, *S. cerevisiae*, and human cells. Biochemical characterization of wild-type and hAAG mutant enzymes and determination of their ability to induce the mutator phenotype in a range of *S. cerevisiae* strains provides important insights into the mechanism of hAAG-induced genomic instability. It turns out that wild-type and mutant hAAGs specifically bind to the DNA containing one and two base-pair loops within repetitive sequences, and the strength of such binding correlates with the extent of frameshift mutagenesis and MSI.

RESULTS

Selection of hAAG Mutant Whose Expression Increases Spontaneous Mutation

In order to identify mutants of hAAG that can significantly elevate spontaneous mutation, wild-type *AAG* cDNA was cloned into the pTrcHis plasmid and randomly mutated at eight of the nine residues lining the active site pocket with the exception of Glu125 residue required for catalysis (Figure 1). The random library contained one or more amino acid substitutions per molecule. The mutated *hAAG* cDNAs were expressed in *E. coli* and enriched for mutator variants using sequential rounds of Rif^R selection. Rif^R colonies were isolated from the population with the notion that Rif^R cells expressing mutator glycosylases would be preferentially recovered from this population. Among the different mutants isolated, an *AAG* cDNA with two amino acid substitutions, Y127I and H136L, was shown to significantly elevate Rif^R mutation frequency above wild-type levels (Figure S1 available online). The cDNA of the Y127I/H136L double mutant was subsequently cloned into different expression vectors for further analysis.

Wild-Type AAG and AAG-Y127I/H136L Increase Spontaneous Frameshift Mutations in *S. cerevisiae*

We tested the effects of expressing both wild-type AAG and AAG-Y127I/H136L on the rate of spontaneous mutation in *S. cerevisiae* (Figures 2A and 2B). *hAAG* cDNAs were cloned into the galactose-inducible pYES vector, and proteins were expressed in various *S. cerevisiae* strains to monitor spontaneous mutation. In addition to base-pair substitutions monitored at *trp1-289* of the BGY strains, we also monitored −1 and +1 frameshift mutations within $(A)_{12}$ and $(A)_{14}$ runs in the *lys2* locus, respectively (Tran et al., 1997). In our previous work, the expression of hAAG in wild-type *S. cerevisiae* did not significantly increase base-pair substitution mutation rates (Glassner et al., 1998b). Similarly, expression of AAG-Y127I/H136L also failed to elevate the base-pair mutation rates at the *trp1-289* locus (data not shown). However, in agreement with a previous report (Hofseth et al., 2003), we observed a modest increase in −1 and +1 frameshift mutation rates by the expression of wild-type AAG in wild-type *S. cerevisiae*. Upon expression of AAG-Y127I/H136L, we observed more than a 100-fold increase in the rate of −1 frameshifts (Figure 2A) and ~14-fold increase in the rate of +1 frameshifts (Figure 2B) over the background.

hAAG-Induced Spontaneous Mutation Differs Mechanistically from that of Mag1

The elevated expression of the yeast Mag1 DNA glycosylase was previously shown to increase the rates of spontaneous base-pair substitutions at the *trp1-289* locus by about 20-fold in wild-type *S. cerevisiae* and by more than 300-fold in the

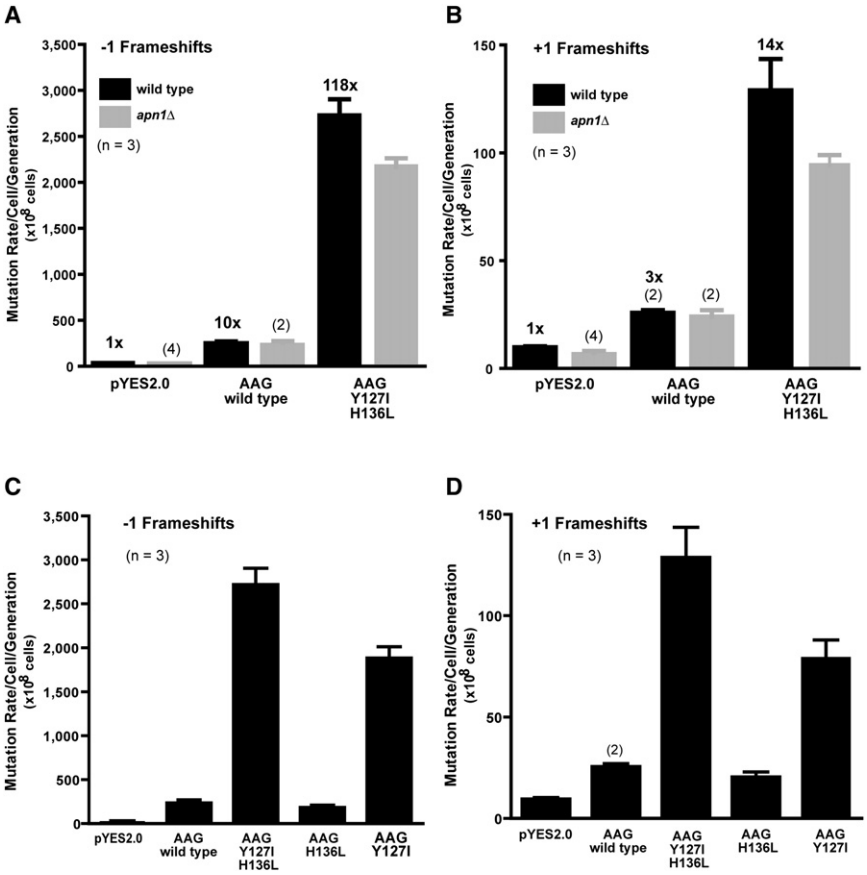

Figure 2. AAG-Y127I/H136L and AAG-Y127I Create Mutator Phenotype in Yeast above the Levels of Wild-Type AAG

(A–D) *hAAG* cDNAs were expressed from pYES2.0 vector and grown as described (Rusyn et al., 2007). Mutation rates in wild-type (black) and *apn1*Δ yeast (gray) for (A) −1 frameshifts and (B) +1 frameshifts. The differences in mutation rates observed between hAAG and AAG-Y127I/H136L are statistically significant, as determined with Student's t test. Differences in mutation rates created by these glycosylases in wild-type and *apn1*Δ yeast are not statistically significant. Mutation rates contributed by AAG-H136L and AAG-Y127I substitutions for (C) −1 frameshifts and (D) +1 frameshifts. The n values for most bars in all panels are equal to 3 (n = 3), except where indicated with the n value mentioned in parentheses above. Error bars represent SEM.

absence of AP endonuclease (Apn1) (Glassner et al., 1998b). Further, the coexpression of Apn1 with Mag1 suppressed the elevated mutation rate, suggesting that it is the unprocessed AP sites generated by Mag1 that increase base-pair substitutions (Glassner et al., 1998b; Rusyn et al., 2007). We tested whether hAAG-induced frameshift mutations might also result from unrepaired AP sites by expressing the wild-type AAG and AAG-Y127I/H136L proteins in the *apn1Δ* background (Figures 2A and 2B). In this case, the absence of Apn1 did not amplify the mutator phenotype induced by hAAG proteins for both −1 frameshift (Figure 2A) and +1 frameshift mutations (Figure 2B); this agrees with a previous observation that the coexpression of Apn1 with hAAG does not suppress frameshift mutagenesis (Hofseth et al., 2003). Taken together, these results suggest that AP sites are not the critical intermediates of hAAG-induced frameshift mutagenesis and that hAAG-induced spontaneous mutagenesis differs mechanistically from that of Mag1.

Y127I Substitution Confers a Strong Frameshift Mutator Phenotype

In order to understand the relative contributions of each amino acid substitution to the observed mutator phenotype conferred by AAG-Y127I/H136L, the single mutants, AAG-Y127I and AAG-H136L, were each expressed in *S. cerevisiae*, and both −1 and +1 frameshift mutation rates were monitored. Expression of the AAG-H136L only increased spontaneous frameshift mutation to the same level as that of wild-type AAG (Figures 2C and 2D). In contrast, AAG-Y127I induced a much stronger mutator phenotype compared to that of both wild-type AAG and AAG-H136L, increasing the rates of spontaneous −1 frameshifts by ~80-fold and +1 frameshifts by more than 8-fold over the background (Figures 2C and 2D). Thus, the AAG-Y127I amino acid substitution accounts for the majority of the increased frameshift mutator phenotype induced by AAG-Y127I/H136L.

Expression of Mutant hAAG Glycosylases Increases Microsatellite Instability in Cultured Human K562 Cells

Having established that the expression of wild-type AAG, AAG-Y127I/H136L, and AAG-Y127I in *S. cerevisiae* gives rise to increased frameshift mutation, we further tested the ability of these AAG proteins to induce genomic instability in cultured human K562 cells (Table 1) after ~40 population doublings. Genomic DNA was isolated after this expansion and subjected to MSI genotyping analysis at five canonical, NCI-recommended microsatellite sites (Table 1). In addition, the *BAT40* locus located within the TGF-β type II receptor gene was monitored for microsatellite instability (MSI). We previously demonstrated that increased levels of wild-type AAG in human cells result in low-level MSI (MSI-L) with instability at the *D2S123* locus (one out of the five NCI loci) and additionally at the *BAT40* locus (Hofseth et al., 2003). We found the same MSI-L phenotype in this study (Table 1). In agreement with results from *S. cerevisiae*, the expression of AAG-Y127I/H136L and AAG-Y127I in K562 cells induced an even stronger mutator phenotype, the high microsatellite instability (MSI-H) with changes at the *D5S346 and D2S123* loci and additionally at *BAT40* (Table 1). Taken together, our results suggest that the expression of hAAG proteins in both *S. cerevisiae* and human K562 cells leads to genomic instability.

Table 1. Expression of hAAG Glycosylases in K562 Human Cells Induced MSI

Microsatellite Marker							
Expressed Protein	*BAT25*	*BAT26*	*D17S250*	*D5S346*	*D2S123*	Phenotype	*BAT40*
Empty vector	–	–	–	–	–	MSS	–
AAG wild-type	–	–	–	–	+	MSI-L	+
AAG-Y127I/H136L	–	–	–	+	+	MSI-H	+
AAG-Y127I	–	–	–	+	+	MSI-H	+

Five NCI-recommended markers were analyzed for MSI (*BAT25* through *D2S123*). If these markers were not found changed from control after the expression period, the phenotype was classified as microsatellite stable (MSS). If one of these five markers was observed with altered nucleotide lengths, the phenotype was classified as low microsatellite instability (MSI-L; wtAAG at the *D2S123*). Finally, if two or more markers were found changed from controls, the phenotype was classified as high microsatellite instability (MSI-H; AAG-Y127I and AAG-Y127I/H136L at *D5S346* and *D2S123*). In addition, *BAT40* was analyzed, as it is analogous to *lys2* poly-A runs of *S. cerevisiae*.

The Mutant hAAG Enzymes Have Reduced DNA Glycosylase Activity

As one measure of the ability of hAAG and its mutants to repair alkylated DNA base lesions, we assessed their ability to protect *S. cerevisiae mag1Δ* cells against methylmethanesulfonate (MMS)-induced cytotoxicity, using in vivo complementation (Figure 3A). This assay primarily provides an estimation of glycosylase-mediated repair of the cytotoxic 3MeA DNA lesion. It should be noted that hAAG can also excise 7MeG lesions but that 7MeG is not considered to be cytotoxic. Upon MMS exposure, both wild-type AAG and AAG-H136L provided the same level of protection in the *mag1Δ* strain, indicating that these enzymes have equivalent capacities for 3MeA repair. In contrast, cells expressing AAG-Y127I showed only partial rescue relative to that of cells expressing wild-type AAG, and AAG-Y127I/H136L completely failed to rescue *mag1Δ* yeast from the MMS-induced cytotoxicity. Given that AAG-H136L behaves similarly to wild-type AAG for both glycosylase activity and mutator activity, we did not biochemically analyze this protein any further.

The results from the in vivo complementation assays for MMS sensitivity were supported by in vitro DNA glycosylase activity

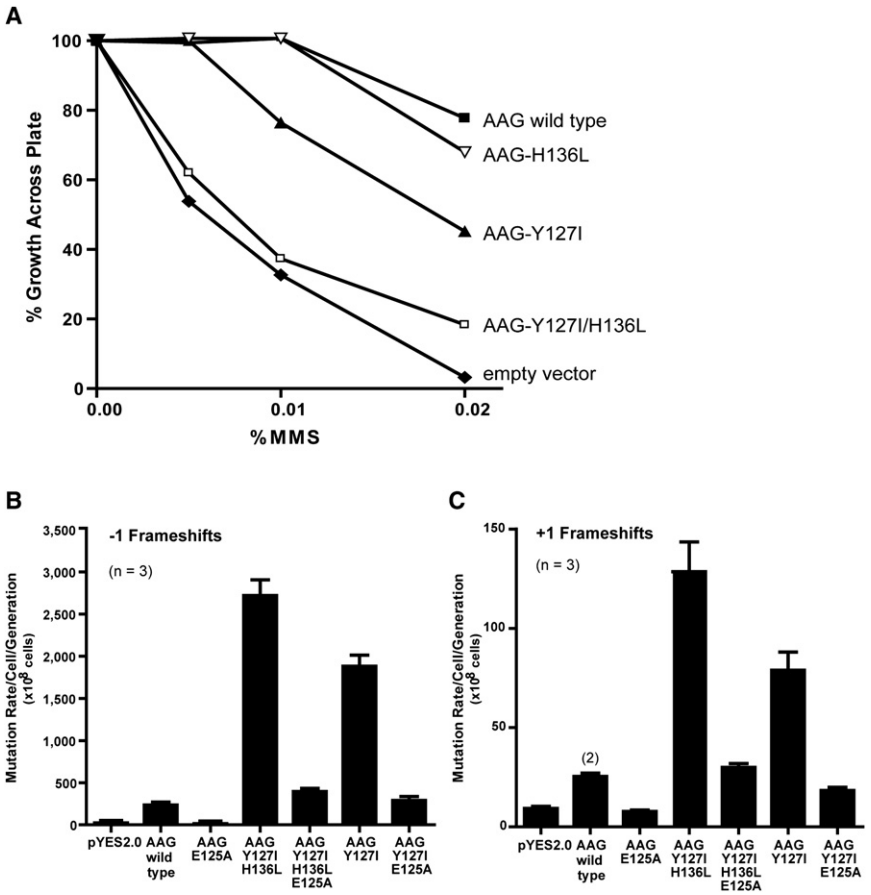

Figure 3. In Vivo Characterization of AAG-Y127I and AAG-Y127I/H136L

(A–C) (A) In vivo complementation assay showing the ability of hAAGs to rescue the *mag1*Δ yeast against different concentrations of MMS incorporated in YPD plates. Percent growth across MMS gradient obtained with empty vector in *mag1*Δ is represented as filled diamond (◆), *mag1*Δ yeast complemented with wtAAG are represented as filled squares (■), AAG-H136L as inverted empty triangles (∇), AAG-Y127I as filled triangles (▲), and AAG-Y127I/H136L as empty squares (□). E125A substitution significantly diminishes, but does not abolish, the ability of AAG-Y127I and AAG-Y127I/H136L to elevate (B) −1 frameshifts and (C) +1 frameshifts. Mutation rates in wild-type yeast generated by AAG-Y127I/E125A and AAG-Y127I/H136L/E125A are statistically significant compared to rates with an empty vector. The n values for most bars in both (B) and (C) are equal to 3, except for one bar in (C). Error bars represent SEM.

Table 2. The Excision Rate Constants and Binding Affinity of hAAG with Standard Deviation Tested for Different DNA Lesions Using Purified hAAG

	k_{obs} ± SD (min^{-1})			K_d ± SD (nM)		
Substrates	AAG Wild-Type	AAG-Y127I	AAG-Y127I/H136L	AAG Wild-Type	AAG-Y127I	AAG-Y127I/H136L
3MeA[a]	0.27 ± 0.05	0.19 ± 0.04	ND**	NA	NA	NA
7MeG[a]	0.06 ± 0.01	ND**	ND**	NA	NA	NA
Hx	0.42 ± 0.05	ND**	ND**	NA	NA	NA
εA	0.11 ± 0.01	0.032 ± 0.007**	ND**	23.9 ± 2.4	31.5 ± 3.9*	114.8 ± 32.3**
AP site	NA	NA	NA		21.1 ±4.5	376.9 ± 98.3**
Poly A loop A	ND	ND	ND	251.3 ± 64.2	98.5 ± 18*	43.95 ± 8.2**

Refer to Figure S4 for raw data used to calculate K_d constants presented in this table. ND, no detectable activity (corresponds to $k_{obs} \leq 0.00002$ min−1 and < 0.0006 fmol/min); *, **, significantly different compared to WT at $p < 0.05$ or $p < 0.01$, respectively; NA, the experiment was not performed.
[a] Measurement units: fmol/min.

assays. Wild-type AAG efficiently removed 3MeA and 7MeG at the rates of 0.27 ± 0.05 and 0.06 ± 0.01 fmol/min, respectively (Table 2). In contrast, the activity of AAG-Y127I/H136L (Table 2) for both 3MeA and 7MeG removal was not detected, accounting for its total failure to protect against MMS-induced cytotoxicity (Figure 3A). In contrast, AAG-Y127I showed intermediate activity for the removal of 3MeA at the rate of 0.19 ± 0.04 fmol/min and showed no detectable activity for 7MeG removal (Table 2). This explains the partial rescue provided by AAG-Y127I mutant against MMS cytotoxicity.

We further studied the ability of hAAG and its mutants to excise Hx and εA and their ability to bind AP site-containing DNA (Table 2). The excision rate for the removal of Hx was robust for the wild-type AAG, with $k_{obs} = 0.42 \pm 0.05$ min^{-1}; in comparison, AAG-Y127I and AAG-Y127I/H136L completely failed to excise this lesion (Table 2). Whereas wild-type AAG removed εA at the rate of $k_{obs} = 0.11 \pm 0.01$ min^{-1}, AAG-Y127I showed significantly reduced activity for εA, with $k_{obs} = 0.032 \pm 0.007$ min^{-1}, and the activity of AAG-Y127I/H136L for εA lesions was undetectable (Table 2). Surprisingly, in spite of their difference in εA excision activity, both wild-type AAG and AAG-Y127I bound the DNA duplex containing an εA lesion with roughly equal affinity, with K_ds of 23.9 and 31.5 nM, respectively. Even though the excision of εA by AAG-Y127I/H136L was not detectable, it bound the εA containing DNA with a significant affinity, $K_d = 114.8 \pm 32.3$ nM (Table 2). Similar to εA, both wild-type AAG and AAG-Y127I bound the AP site containing DNA with roughly equal affinity. However, compared to wild-type AAG, AAG-Y127I/H136L showed ~18-fold reduced affinity for binding the AP site containing DNA.

The Glu125 Catalytic Residue Is Required for hAAG's Frameshift Mutator Phenotype

The fact that the ability of the hAAG mutants to induce frameshift mutagenesis increased with decreasing DNA glycosylase activity led us to question whether base excision is actually required for the observed mutator phenotype. We therefore mutated the catalytic residue Glu125 (to Ala) in the wild-type and mutant hAAG enzymes. Previous studies showed that E125Q and E125A mutants of hAAG show undetectable glycosylase activity and that both bind efficiently to lesion-containing DNA duplex (Abner et al., 2001; O'Brien and Ellenberger, 2003). We also observed that, like AAG-Y127I (Table 2), AAG-Y127I/E125A efficiently binds εA, but, unlike AAG-Y127I, it fails to remove this lesion from the DNA duplex (data not shown). In order to understand the role of Glu125 in the hAAG-induced mutator phenotype, AAG-E125A, AAG-Y127I/E125A, and AAG-Y127I/H136L/E125A mutants were expressed in *S. cerevisiae*, and their ability to increase frameshift rates was monitored. The results in Figures 3B and 3C show that the introduction of the E125A substitution abolished the ability of wild-type AAG to increase both −1 and +1 frameshift mutations. Moreover, the mutator ability of both AAG-Y127I/H136L and AAG-Y127I mutants was also reduced upon replacement of the catalytic Glu125, albeit not completely abolished, indicating that catalytic activity is not the only factor contributing to the observed mutator phenotype. The residual increase in mutation rates for AAG-Y127I/H136L/E125A compared to the empty vector was ~17-fold for −1 frameshifts (Figure 3B) and ~3-fold for +1 frameshifts (Figure 3C). AAG-Y127I/E125A behaved in a similar manner to the triple mutant, being largely suppressed for mutator activity but still increasing the rate of −1 frameshifts by more than 12-fold and +1 frameshift rates by ~2-fold, compared to the empty vector. These results clearly show that the catalytic Glu125 residue is essential for the mutator phenotype induced by wild-type AAG and that it is required for most, but not all, of the mutator phenotypes induced by the hAAG mutants.

The Role of DNA Polymerases in the hAAG-Induced Mutator Phenotype

We tested whether different translesion synthesis (TLS) and replicative DNA polymerases modulate hAAG-induced frameshifts. In *S. cerevisiae*, there are two major TLS polymerases: Polζ, composed of Rev3 and Rev7, and Polη/Rad30. Rev3 is the catalytic subunit of Polζ, and Rev7 is its accessory factor required for bypass activity; Polζ together with Rev1 forms a complex required for TLS (Acharya et al., 2006; Prakash et al., 2005). hAAG proteins were expressed in *rev3*Δ, *rev7*Δ, and *rad30*Δ yeast strains, and frameshift rates were monitored (Figures S2A and S2B). We previously showed that Polζ and Rev1 are required for Mag1-induced base-pair substitutions by facilitating replication and elongation past Mag1-induced AP

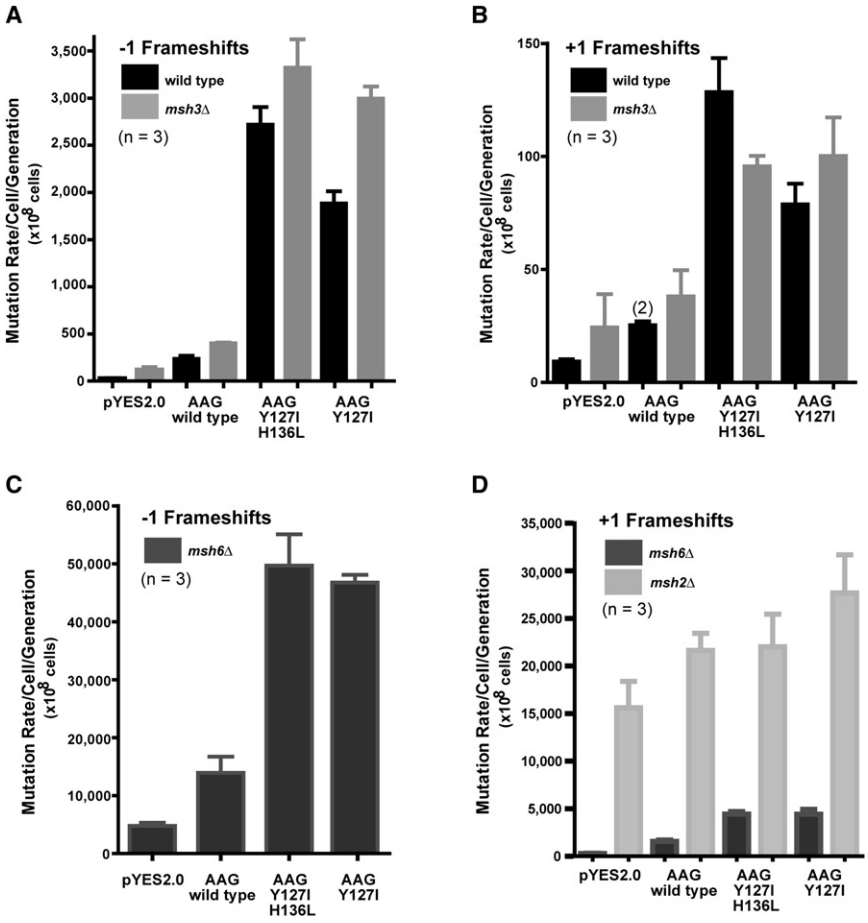

Figure 4. Role of DNA Mismatch Repair in hAAG-Induced Frameshift Mutations

(A–D) Mutation rates observed in wild-type yeast are represented in black and those in MMR-deficient yeast, in gray. Mutation rates determined in *msh3*Δ yeast for hAAG-induced (A) −1 frameshifts and (B) +1 frameshifts. Similarly, hAAG-induced mutation rates determined for (C) −1 frameshifts in *msh6*Δ yeast and (D) +1 frameshifts in *msh6*Δ and *msh2*Δ yeast. The n values for the most bars in all graphs are equal to 3, except for one bar in (B). Error bars represent SEM.

sites (Glassner et al., 1998b). Here, the inactivation of Polζ had no significant effect on the −1 and +1 frameshift rates generated by hAAG proteins. These results once again indicate that there is a clear mechanistic difference between the hAAG- and Mag1-induced spontaneous mutator phenotypes in *S. cerevisiae*. Of interest, in the absence of Rad30, there was a nonsignificant trend toward increasing the rate of −1 frameshifts (Figure S2A) and no significant change in +1 frameshifts. Together, the results showed that Polζ and Polη do not significantly contribute to the observed hAAG-induced mutator phenotype.

Because inactivation of the major TLS polymerases did not significantly affect hAAG-induced frameshifts, we investigated the role of other possible polymerases. Three candidates in *S. cerevisiae* are Rev1, Polδ's Pol32 subunit, and Pol4 (Gibbs et al., 2005; Kalinowski et al., 1995; Shimizu et al., 1993). Rev1 is a deoxycytidyl transferase that forms a complex with Polζ and interacts with ubiquitinated PCNA present at stalled replication forks (Garg and Burgers, 2005). Pol32 is the smallest subunit of Polδ that is thought to play a role in Polδ's processivity and DNA repair activity, linking DNA replication with error-prone, Rad6-dependent translesion bypass (Huang et al., 2000). Finally, Pol4 has been shown to have an intrinsic 5′-deoxyribose phosphate (5′-dRP) lyase activity and is a homolog of mammalian Polβ that has a role in base excision repair (Bebenek et al., 2005; Shimizu et al., 1993). Upon expression of AAG-Y127I/H136L and AAG-Y127I, −1 frameshifts increased to varying extents in the absence of Rev1, Pol32, and Pol4 (Figure S2C). In stark contrast, expression of AAG-Y127I/H136L and AAG-Y127I in the absence of Rev1, Pol32, and Pol4 displayed reduced +1 frameshift rates, compared to wild-type yeast (Figure S2D). Overall, our results suggest that Rev1, Pol4, and Pol32 each suppress hAAG-induced −1 frameshifts but contribute to +1 frameshift mutations in vivo.

Role of Postreplicative DNA Mismatch Repair in hAAG-Induced Frameshifts

The accumulation of frameshifts in vivo is known to be influenced by the postreplication DNA mismatch repair (MMR) pathway (Greene and Jinks-Robertson, 2001; Tran et al., 1997). MMR is initiated either by the MutSα complex (the MSH2-MSH6 heterodimer) binding single base-pair (bp) mismatches or 1 bp loops or by the MutSβ complex (the MSH2-MSH3 heterodimer) binding bp loops ≥ 1 (Kunkel and Erie, 2005). It seemed plausible that hAAG expression in yeast might somehow interfere with MMR activity and that such interference was responsible for hAAG's frameshift mutator phenotype. We reasoned that, if hAAG-induced frameshifts relied solely on inhibiting or depleting MMR activity, then the expression of hAAG proteins in MMR deficient strains should not be able to further affect spontaneous frameshift mutagenesis. The hAAG proteins were thus expressed in *msh6*Δ (MutSα-deficient), *msh3*Δ (MutSβ-deficient), and *msh2*Δ (MutSα- and MutSβ-deficient) yeast strains, and frameshift rates were monitored (Figure 4). In agreement with previous studies (Clark et al., 1999; Tran et al., 1997), the *msh3*Δ deletion had a modest effect on spontaneous frameshifts, *msh6*Δ had a greater effect, and *msh2*Δ had the greatest effect, with ~1700-fold increase in the rate of +1 frameshifts over wild-type. When expressed in the *msh3*Δ and *msh6*Δ yeast strains, wild-type AAG induced a moderate increase in both −1 and +1 frameshift rates, whereas AAG-Y127I and AAG-Y127I/H136L induced even higher increases (Figure 4). Thus, in the absence of either MutSα or MutSβ, the hAAG proteins are still capable of inducing robust −1

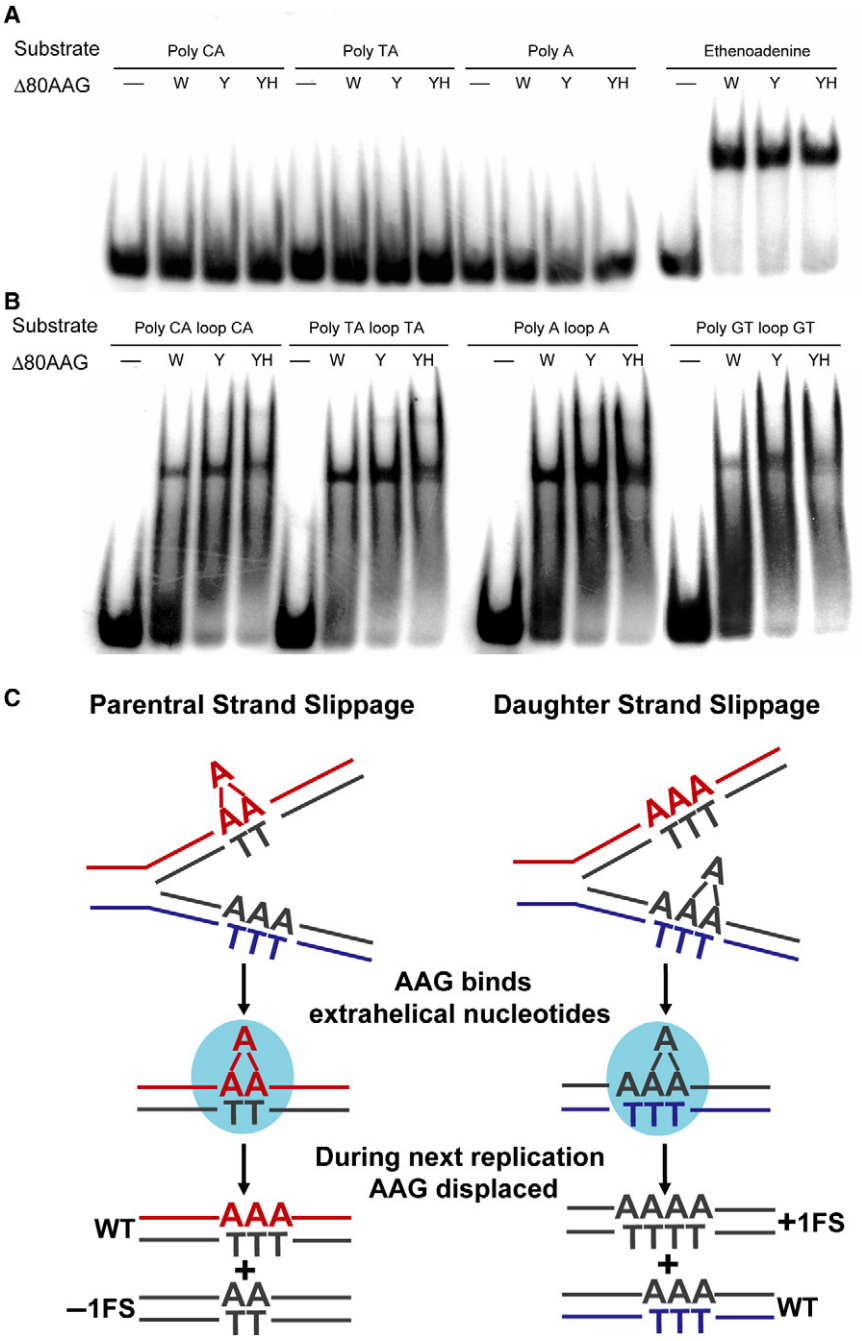

Figure 5. Binding of hAAG Proteins to Base-Pair Loops within Repetitive DNA Sequences

(A and B) Δ80hAAG proteins, in which the first 80 nucleotides from the N terminus were deleted, were incubated at 150 nM with labeled oligos at 4°C and resolved on 5% native-PAGE. Wild-type AAG (W), AAG-Y127I (Y), and AAG-Y127/H136L (YH) were incubated with (A) oligos containing εA and repetitive sequence that do not contain bp loops; (B) indicated loop-containing oligos (see Figure S3 for sequences).

(C) Model for hAAG-induced +1 and −1 frameshift mutations (FS).

and +1 frameshift mutator phenotypes with the same relative strengths. However, because MutSα and MutSβ overlap in their ability to bind 1 bp loop substrates, we went on to monitor hAAG-induced +1 frameshift mutation in the *msh2*Δ (MutSα- and MutSβ-defcient) yeast strain. (Note that, because the *msh2*Δ strain displayed a 50,000-fold increase in −1 frameshift mutagenesis compared to wild-type [Tran et al., 1997], it was not included in this part of the study.) Despite the high background of +1 frameshift mutation rate in the *msh2*Δ strain of ~15,000 × 10^{-8}/generation, expression of the hAAG proteins further enhanced this rate by an extra 7,000 to 12,000 × 10^{-8}/generation (Figure 4D). These results demonstrate that simple inhibition or depletion of the major MMR pathways is not sufficient to explain the hAAG-induced mutator phenotype and, more importantly, that there exists an MMR-independent mechanism that contributes to hAAG-induced frameshift mutagenesis and microsatellite instability.

Interaction of hAAG and Its Mutants with Different One and Two Base-Pair Loops

We went on to test whether hAAG and its mutants could recognize bp loops that are thought to arise from polymerase slippage in microsatellite sequences. We chose substrate sequences analogous to those that showed the MSI-H phenotype in human K562 cells: poly-CA repeats in *D5S346* and *D2S123*, poly-TA repeats in *D2S123*, and poly-A/T repeats present in *BAT-40* as well as in the *S. cerevisiae lys2* loci. We tested the interaction of hAAG proteins with oligos containing CA, TA, A, GT, or T bp loops located within their respective repeats (Figures 5 and S3). Binding assays showed that all three hAAG proteins specifically bind CA, TA, A, and GT bp loop-containing oligos (Figure 5B), displaying no binding to the same oligos without loops (Figure 5A). The hAAG proteins also weakly bound to T bp loops (data not shown). The quantification of the binding affinity to the critical poly-A loop A oligo showed that AAG-Y127I/H136L binds this loop with a high affinity of 43.95 ± 8.2 nM, whereas AAG-Y127I binds the loop with an affinity of 98.5 ± 18 nM that is ~2-fold reduced (Table 2). In contrast, wild-type AAG bound poly-A loop A oligo with significantly reduced affinity of 251.3 ± 64.2 nM that is ~6-fold reduced compared to AAG-Y127I/H136L (Table 2). The binding affinity of hAAG proteins is thus

positively correlated with their ability to induce frameshift mutations in vivo; in other words, the higher the binding affinity to the poly-A loop A oligo in vitro, the higher the induced frameshift mutator phenotype. We tested whether the hAAG proteins can remove normal bases from the one and two bp loops to which they bind; all three hAAG proteins failed to remove normal bases from loop-containing oligos (data not shown); note that we can not eliminate the possibility that base excision may occur in vivo. Importantly, we found that AAG-E125A and AAG-Y127I/E125A failed to bind the poly-A loop A-containing oligo (data not shown). It is important to point out here that the E125A mutant does not lose the ability to flip εA into its active site but does lose the ability to excise this base; however, E125A (and Y127/E125A) simply does not bind the DNA-containing poly-A loop A. This explains, at least in part, the observation that E125A mutants of AAG and AAG-Y127I were compromised in their ability to elevate frameshift mutation (Figures 3B and 3C). Taken together, these results suggest that hAAG proteins specifically bind the one or two bp loops that are expected to form at DNA microsatellites as a result of polymerase replication slippage and that such binding is responsible for the frameshift mutator and MSI phenotype conferred by these proteins (Figure 5C).

DISCUSSION

DNA microsatellites are comprised of repetitive nucleotide sequences that constitute about 30% of the human genome. Microsatellites have been reported to be hot spots for recombination, DNA polymerase slippage, and random DNA integration. Changes in repetitive sequences can result in deleterious effects on gene function leading to adverse phenotypic effects (Atkin, 2001; Boland et al., 2008). Microsatellite instability results from small deletions or expansions within polynucleotide repeats in genomic DNA, and frameshift mutations (−1 or +1) represent the most common mutations associated with MSI. Frameshifts are thought to result from DNA polymerase slippage and strand misalignment during replication (Debrauwere et al., 1997; Kunkel and Bebenek, 2000). An increase or decrease in the repeat length could occur if the slippage is on the daughter or on the template strand, respectively (Boland et al., 2008). Such replication slippage intermediates would have to either be misrepaired or persist until the next round of DNA replication in order for frameshift mutations to be fixed. Proteins that specifically bind and stabilize replication slippage intermediates, thus interfering with their repair, could clearly enhance both frameshift mutagenesis and MSI (Figure 5C).

In humans, MSI has been closely associated with many diseases, including cancer and other disorders that exhibit a dominant mode of inheritance, such as spinal and bulbar muscular dystrophy, Huntington's disease, spinocerebellar ataxia type I, insulin-dependent diabetes mellitus, Friedrich's ataxia, Myotonic dystrophy, Fragile X syndrome, Jacobsen 11q-deletion syndrome, and so on (Debrauwere et al., 1997). It has been shown that the majority of tumors in hereditary nonpolyposis colorectal cancer (HNPCC), sporadic colorectal, and gastric and endometrial cancers are associated with microsatellite length alterations, termed high-frequency microsatellite instability (MSI-H) (Imai and Yamamoto, 2008). HNPCC results primarily from germline mutations in one of the DNA MMR genes, primarily in *MLH1* or *MSH2* in HNPCC and ovarian tumors and less so in *MSH6* and *PMS2* (Imai and Yamamoto, 2008; Parsons et al., 1995a; Plotz et al., 2006). The key function of MMR is to eliminate base mismatches and insertion/deletion loops arising during DNA replication from polymerase slippage (Kunkel and Erie, 2005). The genetic and epigenetic inactivation of MMR genes predisposes to cancer development. Correspondingly, in yeast, frameshift errors at repetitive sequences increase by 10- to 100-fold in MMR-deficient cells relative to controls (Harfe and Jinks-Robertson, 2000; Tran et al., 1997). In this study, we find evidence for an alternative pathway for the induction of frameshift mutations and microsatellite instability that is independent of MMR.

We previously found that elevated expression of hAAG increases spontaneous frameshift mutagenesis in yeast and confers a low-frequency MSI (MSI-L) phenotype in human cells. Here, we report the isolation and characterization of an hAAG mutant AAG-Y127I/H136L with an enhanced ability for spontaneous mutation in *E. coli*, yeast, and human cells. Tyr127 and His136 are highly conserved and important residues in hAAG's active site. Previous studies have assessed the tolerance of hAAG's active site residues for random substitutions and the essentiality of these residues for survival after DNA methylation damage (Chen et al., 2008; Guo et al., 2004). When selecting for MMS resistance in *E. coli*, Tyr127 and His136 show very low substitutability, underscoring their importance in hAAG-mediated excision of cytotoxic 3MeA DNA lesions. Another study tested the importance of active site residues using genetic complementation assay for the rescue of MMS sensitivity in *mag1*Δ yeast cells (Lau et al., 2000); whereas AAG-Y127F provided a partial resistance to MMS, AAG-H136Q provided complete resistance to MMS. Similarly, we find that AAG-Y127I provided partial resistance to MMS and that AAG-H136L provided almost complete resistance to MMS in *mag1*Δ yeast (Figure 3A). Of interest, AAG-Y127I/H136L completely failed to rescue *mag1*Δ cells from MMS-induced sensitivity (Figure 3A), presumably due to its inability to remove MMS-generated 3MeA lesions (Table 2).

The effects of Y127I and H136L substitutions on hAAG's damage base removal can be understood from structural studies of hAAG-DNA complexes (Lau et al., 2000). In the crystal structure of hAAG-DNA complexes, εA base is stacked between Tyr127 and His136 residues (Figure 1). Tyr127 also donates a hydrogen bond to the catalytic Glu125. His136 forms hydrogen bonds from its main chain amide to the N6 of εA, through its side chain to the 5′ phosphate of εA, and with the Tyr157 side chain (Figure 1). When the Y127I and H136L mutations are modeled into the hAAG active site, Ile127 significantly lacks the ability to stack εA and fails to hydrogen bond to Glu125. Leu136 maintains the possibility of hydrogen bonding to N6 of εA through its main-chain amide but fails to form hydrogen bonds to 5′ phosphate of εA and Tyr157 side chain (Figure 1).

Previous biochemical studies showed that hAAG recognizes purine and pyrimidine mismatches that represent one set of MMR substrates and can excise the undamaged purines, but not pyrimidines, from these mismatches (Biswas et al., 2002;

O'Brien and Ellenberger, 2003; O'Brien and Ellenberger, 2004a). Our study now reports that hAAG recognizes another set of MMR substrates, namely one and two bp loops that are generated at microsatellites by DNA polymerase slippage and are prime substrates for MMR. We now know that hAAG and its variants can bind these bp loops and greatly increase the chance that the base-pair loops will be fixed into frameshift mutations. It seems likely that bp loop repair could be inhibited simply by shielding them from MMR. However, hAAG and its mutants are able to induce frameshift mutagenesis even in the absence of MMR, albeit to a limited extent, indicating that whereas shielding bp loops from MMR is highly likely to be involved, it can not solely account for hAAG's mutator activity. We propose that hAAG binding stabilizes bp loops such that they persist until the next round of DNA replication and that such stabilized loops induce frameshift mutations and microsatellite instability. Indeed, the increase in the rate of +1 and −1 frameshift mutations by the hAAG proteins corresponds well with their binding affinity for the 1 bp loop in poly-A-containing DNA (Figures 4 and 5, Table 2). Of interest, hAAG-induced frameshifts are influenced by Rev1, Pol4, and Pol32; in the absence of these polymerases, mutant hAAG-expressing cells exhibit increased −1 frameshifts and decreased +1 frameshifts. We infer that these polymerases are involved in either facilitating or suppressing strand elongation from the looped out primer-template structures (see Figure 5C); when present, the polymerases presumably suppress elongation from daughter strands paired with a slipped parental strand (thus decreasing −1 frameshifts) and facilitate elongation from a daughter strand that has slipped relative to its template (thus increasing +1 frameshifts). Despite their binding to one and two bp loops, hAAG and its mutants were unable to remove normal bases from these loops to produce abasic sites; this perhaps explains the fact that modulating AP-endonuclease activity and eliminating translesion DNA polymerase activities did not influence hAAG-induced frameshifts (Figure 2).

Taken together, our results provide evidence for an additional mechanism for hAAG-induced genomic instability. Elevated expression of hAAG and its variants induces frameshift mutagenesis and MSI by binding to and stabilizing bp loops and shielding them from repair both in the presence and the absence of the MMR pathway. Such hAAG-induced frameshift mutagenesis and MSI is highly likely to contribute to an increased risk of cancer, such as that observed in ulcerative colitis patients.

EXPERIMENTAL PROCEDURES

Plasmids

Table S1 shows all plasmids used in this study.

Strains

Table S2 shows all *E. coli* and *S. cerevisiae* strains used in this study. Most yeast strains were derived from E133 and E134 (Tran et al., 1997) and created by introduction of appropriate *kanMX4* cassette according to standard protocols (Supplemental Experimental Procedures).

Selection of AAG-Y127I/H136L Mutant in *E. coli*

A large library of mutant *hAAG* cDNAs with substitutions targeted to eight active site residues (Tyr127, Ala134, Ala135, His136, Tyr159, Cys167, Asn169, and Leu180) was expressed in *E. coli* (Figure S1). Mutant cDNAs were isolated after several rounds of rifampicin resistance (Rif^R) selection as described in the Supplemental Experimental Procedures. This forward mutation assay mostly scores for base-pair substitutions but also for frameshift mutations (Takechi et al., 2006). A double hAAG mutant with the substitutions Y127I and H136L was isolated.

Determination of Mutation Rates

Spontaneous frameshift mutation rates were determined as previously described (Rusyn et al., 2007), using Drake's method of the median (Rosche and Foster, 2000). Trp^R revertants that score for base-pair substitutions were assayed in the BGY111 strain.

Complementation Assays with hAAG Glycosylases

The *mag1*Δ strain was used to test the ability of the mutant *hAAG* cDNAs to provide alkylation resistance on MMS gradient plates. Overnight cultures were divided into two separate cultures and grown for additional 3 hr at 30°C either uninduced, in 2% glucose, or induced with 2% galactose. Following this initial expression period, cells were mixed with top agar (1%) and stamped onto gradient MMS plates containing either glucose or galactose (Chen et al., 1994). After 3 day incubation at 30°C, growth across the MMS gradient plate was measured for different *hAAG* cDNAs and compared to growth across the gradient for the *mag1*Δ strain carrying the empty vector.

DNA Glycosylase Activity Assays

DNA glycosylase assays were performed essentially as described (Kartalou et al., 2000). Excision of 3MeA and 7MeG from tritiated calf thymus DNA was previously described (Chen et al., 2008). For detailed protocols, refer to the Supplemental Information. The rate constants were calculated by fitting the data to the one-phase exponential function (equation 1) using GraphPad Prism analysis software (GraphPad Software, Inc., La Jolla, CA).

$$Y = Y_{max}\left(1 - e^{-kobs^{*}t}\right) \quad (1)$$

in which Y is the amount of substrate cleaved at any given time point, Y_{max} is the maximum amount of substrate cleaved, t is the time, and k_{obs} is the observed rate constant.

Gel Mobility Shift Assays

Protein-DNA-binding assays were carried out as previously described with slight modifications (Kartalou et al., 2000). For detailed protocol, refer to the Supplemental Information. The binding constants for AAG binding to εA and AP site DNA were calculated by fitting the data to one-site binding (equation 2), using GraphPad Prism analysis software (GraphPad Software, Inc., La Jolla, CA).

$$Y = B_{max}{}^{*}X/(K_d + X) \quad (2)$$

in which Y is the total bound substrate, B_{max} is the maximum specific binding, X is the concentration of the protein, and K_d is the apparent binding constant. The K_d values for AAG binding to poly-A-loop-A substrates were calculated by fitting the data to the following equation (3) for quadratic binding isotherm.

$$F = f_1 \cdot L_o + \frac{1}{2}(f_2 - f_1)\left[(P_o + L_o + K_d) - \sqrt{(P_o + L_o + K_d)^2 - 4 \cdot P_o \cdot L_o}\right] \quad (3)$$

In the above equation, f1 is the signal in the absence of protein, and f2 is the signal at the maximum protein concentration. P_o is the total protein concentration, L_o is the total ligand concentration, and K_d is the dissociation constant (K_d).

Selection of hAAG-Expressing Clones in K562 Cells

pCAGGS vectors with or without *hAAG* cDNAs and selective pMACS-Kk.II (Miltenyi Biotech, Auburn, CA) plasmids were linearized with *Sca* I, ethanol precipitated, and cotransfected into K562 cells with lipofectamine 2000 (Invitrogen) according to manufacturer's instructions. Positive, H-2Kk surface marker-expressing cells were isolated according to manufacturer's instructions and cloned at 0.5 cells per well in 96-well plates. pCAGGS-hAAG clones were screened by PCR for hAAG and assayed for hAAG-expression by western blots and qRT-PCR. For westerns, polyclonal rabbit antibody raised against full-length AAG was used (Covance Research Company, Denver,

PA). mRNA was isolated from ~1 × 10^6 cells with QIAshredder Kit, and cDNA was obtained with Omniscript Reverse Transcriptase Kit (QIAGEN). qRT-PCR was performed with SYBR green method (Applied Biosystems, Foster City, CA). Primers for hAAG PCR and RT-PCR are described in Table S3.

Analysis of MSI

K562 cell lines expressing hAAG glycosylases were cultured as previously described for ~40 population doublings (Hofseth et al., 2003). Genomic DNA was isolated using High Pure PCR Template Preparation Kit (Roche, Burlington, NC) according to manufacturer's instructions. Forward PCR primers (Invitrogen) were fluorescently labeled with FAM dye, and Platinum GenoTYPE *Tsp* DNA Polymerase (Invitrogen) was used. PCR reactions were performed according to manufacturer's instructions with 20 ng template DNA per reaction. Reaction products were run on AB Prism 3738*xl* analyzer at SeqWright facility (Houston, TX), and resulting data from the genotyping chromatograms were aligned and scored for significant changes in microsatellite band length distribution. A set of five markers for MSI was chosen and analyzed with accordance to NCI recommendations (Boland et al., 1998). Additionally, poly(A) *BAT40* locus within the TGF-β type II receptor gene was included (Parsons et al., 1995b).

SUPPLEMENTAL INFORMATION

Supplemental Information includes Supplemental Experimental Procedures, four figures, and three tables and can be found with this article online at doi:10.1016/j.molcel.2010.01.038.

ACKNOWLEDGMENTS

This work was supported by the following grants: CA055042, CA115802, and ES02109. L.D.S. is an American Cancer Society Research Professor.

Received: August 3, 2009
Revised: December 28, 2009
Accepted: January 21, 2010
Published: March 25, 2010

REFERENCES

Abner, C.W., Lau, A.Y., Ellenberger, T., and Bloom, L.B. (2001). Base excision and DNA binding activities of human alkyladenine DNA glycosylase are sensitive to the base paired with a lesion. J. Biol. Chem. *276*, 13379–13387.

Acharya, N., Johnson, R.E., Prakash, S., and Prakash, L. (2006). Complex formation with Rev1 enhances the proficiency of Saccharomyces cerevisiae DNA polymerase zeta for mismatch extension and for extension opposite from DNA lesions. Mol. Cell. Biol. *26*, 9555–9563.

Atkin, N.B. (2001). Microsatellite instability. Cytogenet. Cell Genet. *92*, 177–181.

Bebenek, K., Garcia-Diaz, M., Patishall, S.R., and Kunkel, T.A. (2005). Biochemical properties of Saccharomyces cerevisiae DNA polymerase IV. J. Biol. Chem. *280*, 20051–20058.

Berdal, K.G., Johansen, R.F., and Seeberg, E. (1998). Release of normal bases from intact DNA by a native DNA repair enzyme. EMBO J. *17*, 363–367.

Biswas, T., Clos, L.J., II, SantaLucia, J., Jr., Mitra, S., and Roy, R. (2002). Binding of specific DNA base-pair mismatches by N-methylpurine-DNA glycosylase and its implication in initial damage recognition. J. Mol. Biol. *320*, 503–513.

Boland, C.R., Thibodeau, S.N., Hamilton, S.R., Sidransky, D., Eshleman, J.R., Burt, R.W., Meltzer, S.J., Rodriguez-Bigas, M.A., Fodde, R., Ranzani, G.N., and Srivastava, S. (1998). A National Cancer Institute Workshop on Microsatellite Instability for cancer detection and familial predisposition: Development of international criteria for the determination of microsatellite instability in colorectal cancer. Cancer Res. *58*, 5248–5257.

Boland, C.R., Koi, M., Chang, D.K., and Carethers, J.M. (2008). The biochemical basis of microsatellite instability and abnormal immunohistochemistry and clinical behavior in Lynch syndrome: from bench to bedside. Fam. Cancer *7*, 41–52.

Chen, B.J., Carroll, P., and Samson, L. (1994). The Escherichia coli AlkB protein protects human cells against alkylation-induced toxicity. J. Bacteriol. *176*, 6255–6261.

Chen, C.Y., Guo, H.H., Shah, D., Blank, A., Samson, L.D., and Loeb, L.A. (2008). Substrate binding pocket residues of human alkyladenine-DNA glycosylase critical for methylating agent survival. DNA Repair (Amst.) *7*, 1731–1745.

Clark, A.B., Cook, M.E., Tran, H.T., Gordenin, D.A., Resnick, M.A., and Kunkel, T.A. (1999). Functional analysis of human MutSalpha and MutSbeta complexes in yeast. Nucleic Acids Res. *27*, 736–742.

Debrauwere, H., Gendrel, C.G., Lechat, S., and Dutreix, M. (1997). Differences and similarities between various tandem repeat sequences: minisatellites and microsatellites. Biochimie *79*, 577–586.

Drohat, A.C., Kwon, K., Krosky, D.J., and Stivers, J.T. (2002). 3-Methyladenine DNA glycosylase I is an unexpected helix-hairpin-helix superfamily member. Nat. Struct. Biol. *9*, 659–664.

Fan, J., and Wilson, D.M., III. (2005). Protein-protein interactions and post-translational modifications in mammalian base excision repair. Free Radic. Biol. Med. *38*, 1121–1138.

Friedberg, E.C. (2006). DNA repair and mutagenesis, Second Edition (Washington, D.C.: ASM Press).

Garg, P., and Burgers, P.M. (2005). Ubiquitinated proliferating cell nuclear antigen activates translesion DNA polymerases eta and REV1. Proc. Natl. Acad. Sci. USA *102*, 18361–18366.

Gibbs, P.E., McDonald, J., Woodgate, R., and Lawrence, C.W. (2005). The relative roles in vivo of Saccharomyces cerevisiae Pol eta, Pol zeta, Rev1 protein and Pol32 in the bypass and mutation induction of an abasic site, T-T (6-4) photoadduct and T-T cis-syn cyclobutane dimer. Genetics *169*, 575–582.

Gillen, C.D., Walmsley, R.S., Prior, P., Andrews, H.A., and Allan, R.N. (1994). Ulcerative colitis and Crohn's disease: a comparison of the colorectal cancer risk in extensive colitis. Gut *35*, 1590–1592.

Glassner, B.J., Posnick, L.M., and Samson, L.D. (1998a). The influence of DNA glycosylases on spontaneous mutation. Mutat. Res. *400*, 33–44.

Glassner, B.J., Rasmussen, L.J., Najarian, M.T., Posnick, L.M., and Samson, L.D. (1998b). Generation of a strong mutator phenotype in yeast by imbalanced base excision repair. Proc. Natl. Acad. Sci. USA *95*, 9997–10002.

Greene, C.N., and Jinks-Robertson, S. (2001). Spontaneous frameshift mutations in Saccharomyces cerevisiae: accumulation during DNA replication and removal by proofreading and mismatch repair activities. Genetics *159*, 65–75.

Guo, H.H., and Loeb, L.A. (2003). Tumbling down a different pathway to genetic instability. J. Clin. Invest. *112*, 1793–1795.

Guo, H.H., Choe, J., and Loeb, L.A. (2004). Protein tolerance to random amino acid change. Proc. Natl. Acad. Sci. USA *101*, 9205–9210.

Harfe, B.D., and Jinks-Robertson, S. (2000). DNA mismatch repair and genetic instability. Annu. Rev. Genet. *34*, 359–399.

Hofseth, L.J., Khan, M.A., Ambrose, M., Nikolayeva, O., Xu-Welliver, M., Kartalou, M., Hussain, S.P., Roth, R.B., Zhou, X., Mechanic, L.E., et al. (2003). The adaptive imbalance in base excision-repair enzymes generates microsatellite instability in chronic inflammation. J. Clin. Invest. *112*, 1887–1894.

Hollis, T., Lau, A., and Ellenberger, T. (2000). Structural studies of human alkyladenine glycosylase and E. coli 3-methyladenine glycosylase. Mutat. Res. *460*, 201–210.

Huang, M.E., de Calignon, A., Nicolas, A., and Galibert, F. (2000). POL32, a subunit of the Saccharomyces cerevisiae DNA polymerase delta, defines a link between DNA replication and the mutagenic bypass repair pathway. Curr. Genet. *38*, 178–187.

Imai, K., and Yamamoto, H. (2008). Carcinogenesis and microsatellite instability: the interrelationship between genetics and epigenetics. Carcinogenesis *29*, 673–680.

Kalinowski, D.P., Larimer, F.W., and Plewa, M.J. (1995). Analysis of spontaneous frameshift mutations in REV1 and rev1-1 strains of Saccharomyces cerevisiae. Mutat. Res. *331*, 149–159.

Kartalou, M., Samson, L.D., and Essigmann, J.M. (2000). Cisplatin adducts inhibit 1,N(6)-ethenoadenine repair by interacting with the human 3-methyladenine DNA glycosylase. Biochemistry *39*, 8032–8038.

Kunkel, T.A., and Bebenek, K. (2000). DNA replication fidelity. Annu. Rev. Biochem. *69*, 497–529.

Kunkel, T.A., and Erie, D.A. (2005). DNA mismatch repair. Annu. Rev. Biochem. *74*, 681–710.

Lau, A.Y., Schärer, O.D., Samson, L., Verdine, G.L., and Ellenberger, T. (1998). Crystal structure of a human alkylbase-DNA repair enzyme complexed to DNA: mechanisms for nucleotide flipping and base excision. Cell *95*, 249–258.

Lau, A.Y., Wyatt, M.D., Glassner, B.J., Samson, L.D., and Ellenberger, T. (2000). Molecular basis for discriminating between normal and damaged bases by the human alkyladenine glycosylase, AAG. Proc. Natl. Acad. Sci. USA *97*, 13573–13578.

Lindahl, T. (1993). Instability and decay of the primary structure of DNA. Nature *362*, 709–715.

Lingaraju, G.M., Kartalou, M., Meira, L.B., and Samson, L.D. (2008). Substrate specificity and sequence-dependent activity of the Saccharomyces cerevisiae 3-methyladenine DNA glycosylase (Mag). DNA Repair (Amst.) *7*, 970–982.

O'Brien, P.J., and Ellenberger, T. (2003). Human alkyladenine DNA glycosylase uses acid-base catalysis for selective excision of damaged purines. Biochemistry *42*, 12418–12429.

O'Brien, P.J., and Ellenberger, T. (2004a). Dissecting the broad substrate specificity of human 3-methyladenine-DNA glycosylase. J. Biol. Chem. *279*, 9750–9757.

O'Brien, P.J., and Ellenberger, T. (2004b). The Escherichia coli 3-methyladenine DNA glycosylase AlkA has a remarkably versatile active site. J. Biol. Chem. *279*, 26876–26884.

Parsons, R., Li, G.M., Longley, M., Modrich, P., Liu, B., Berk, T., Hamilton, S.R., Kinzler, K.W., and Vogelstein, B. (1995a). Mismatch repair deficiency in phenotypically normal human cells. Science *268*, 738–740.

Parsons, R., Myeroff, L.L., Liu, B., Willson, J.K., Markowitz, S.D., Kinzler, K.W., and Vogelstein, B. (1995b). Microsatellite instability and mutations of the transforming growth factor beta type II receptor gene in colorectal cancer. Cancer Res. *55*, 5548–5550.

Plotz, G., Zeuzem, S., and Raedle, J. (2006). DNA mismatch repair and Lynch syndrome. J. Mol. Histol. *37*, 271–283.

Posnick, L.M., and Samson, L.D. (1999). Imbalanced base excision repair increases spontaneous mutation and alkylation sensitivity in Escherichia coli. J. Bacteriol. *181*, 6763–6771.

Prakash, S., Johnson, R.E., and Prakash, L. (2005). Eukaryotic translesion synthesis DNA polymerases: specificity of structure and function. Annu. Rev. Biochem. *74*, 317–353.

Rosche, W.A., and Foster, P.L. (2000). Determining mutation rates in bacterial populations. Methods *20*, 4–17.

Rusyn, I., Fry, R.C., Begley, T.J., Klapacz, J., Svensson, J.P., Ambrose, M., and Samson, L.D. (2007). Transcriptional networks in S. cerevisiae linked to an accumulation of base excision repair intermediates. PLoS ONE *2*, e1252.

Shimizu, K., Santocanale, C., Ropp, P.A., Longhese, M.P., Plevani, P., Lucchini, G., and Sugino, A. (1993). Purification and characterization of a new DNA polymerase from budding yeast Saccharomyces cerevisiae. A probable homolog of mammalian DNA polymerase beta. J. Biol. Chem. *268*, 27148–27153.

Takechi, S., Yamaguchi, T., Nomura, H., Minematsu, T., Adachi, M., Kurata, H., and Kurata, R. (2006). Mutation spectrum induced by dihydropyrazines in Escherichia coli. Biol. Pharm. Bull. *29*, 17–20.

Tran, H.T., Keen, J.D., Kricker, M., Resnick, M.A., and Gordenin, D.A. (1997). Hypermutability of homonucleotide runs in mismatch repair and DNA polymerase proofreading yeast mutants. Mol. Cell. Biol. *17*, 2859–2865.

Wyatt, M.D., and Samson, L.D. (2000). Influence of DNA structure on hypoxanthine and 1,N(6)-ethenoadenine removal by murine 3-methyladenine DNA glycosylase. Carcinogenesis *21*, 901–908.

Wyatt, M.D., Allan, J.M., Lau, A.Y., Ellenberger, T.E., and Samson, L.D. (1999). 3-methyladenine DNA glycosylases: structure, function, and biological importance. Bioessays *21*, 668–676.

Xiao, W., and Samson, L. (1993). In vivo evidence for endogenous DNA alkylation damage as a source of spontaneous mutation in eukaryotic cells. Proc. Natl. Acad. Sci. USA *90*, 2117–2121.

Molecular Cell, *Volume 37*

Supplemental Information

Frameshift Mutagenesis and Microsatellite Instability Induced by Human Alkyladenine DNA Glycosylase

Joanna Klapacz, Gondichatnahalli M. Lingaraju, Haiwei H. Guo, Dharini Shah, Ayelet Moar-Shoshani, Lawrence A. Loeb, and Leona D. Samson

Supplemental Experimental Protocols

Description of plasmids used in the study:

For the expression of 3MeA DNA glycosylases in yeast, cDNAs were cloned into the galactose-inducible pYES2.0 expression vector (Invitrogen Corp., San Diego, CA) and confirmed by DNA sequencing (performed at Elim Biopharmeceuticals, San Francisco, CA). Wild-type *hAAG* and *MAG1* containing pYES vectors were from Glassner et al, 1998. For analysis in *E. coli*, *hAAG* cDNAs were cloned into pTrcHis (Invitrogen) and confirmed by sequencing. For protein purification, the expression plasmid was a modified version of pET19b containing an inserted precision protease site (PPS) in front of *hAAG* cDNAs (Lau et al., 1998; Lau et al., 2000). The hAAG-Y127I/H136L double mutant was isolated from a large library generated by oligonucleotide-replacement of the active site residues with random nucleotides. hAAG-Y127I and hAAG-H136L single mutants were created by site directed-mutagenesis of the wild-type cDNA, using the oligonucleotide primers (Invitrogen) that contained point mutations (Supplementary Table 3). The nucleotide sequence of all mutants was confirmed by DNA sequencing. For hAAG cloning into the high-expression eukaryotic pCAGGS plasmid (Niwa et al., 1991), cDNA was PCR amplified from pYES-hAAG containing plasmids (Supplementary Table

3), and PCR product and plasmid were digested with *Xho* I (NEB, MA), ligated and transformed into competent XL10 Gold cells (Stratagene). Isolated plasmids (Mini Kit, QIAGEN) were screened for inserts and for the right orientation with restriction digests and DNA sequencing. For transfection into K562 cells and clone selection, pMACS-Kk.II (Miltenyi Biotech, Auburn, CA) plasmids were co-transfected with pCAGGS vectors with or without *hAAG* cDNAs. Positive, H-2Kk surface-marker expressing cells were isolated according to manufacturer's instructions, cloned and screened by PCR for pCAGGS-hAAG DNA using primers from Supplementary Table 3.

S. cerevisiae strain construction and scoring of frameshift mutants:

Strains E133*apn1Δ*, E134*apn1Δ*, E134*rev7Δ*, E133*rev3Δ* were constructed previously by disruption of the gene with the *HIS3* cassette (Glassner et al., 1998b; Hofseth et al., 2003; Rusyn et al., 2007). All other mutant alleles were derived from the *S. cerevisiae* Gene Deletion Library as follows. *kanMX4* cassette was PCR amplified from the genome of the appropriate strain in the deletion library and transformed into wild type E133 and E134 strains. The resulting deletion strains were confirmed by genomic PCR and by their sensitivity to MMS and other agents. Briefly, overnight cultures were serially diluted by 5-fold and stamped onto MMS-containing YPD plates, grown for 3 days at 30^{o}C and compared to wild-type E133/E134 strains. The *kanMX4* cassettes and pYES vectors were introduced into the yeast strains by way of G418-resistance or uracil auxotrophy, respectively, utilizing Geitz Transformation Kit and protocol. For determination of frameshift mutants, overnight cultures were diluted into 10 parallel cultures at an initial density of 4000 cells/ml. Cultures were grown to saturation at 30^{o}C for 4 days in SC-ura

synthetic media containing 2% galactose (BioGene, CA). +1 and -1 frameshift revertants were scored on SC-lys/agar plates (Glassner et al., 1998), whereas base pair substation mutants were scored on SC-trp/agar plates (Glassner et al., 1998).

Purification of hAAG glycosylases from pET19b-PPS vector:

pET19b-PPS vectors containing recombinant *hAAG* cDNAs were introduced into BL21(DE3) expression cells by the calcium chloride method. Expression was induced by 0.5 μM IPTG in late-exponential cultures and overnight incubation at room temperature. The truncated hAAG constructs were deleted for the N-terminal 80 amino acids to facilitate purification and to improve the solubility as previously described (Lau et al., 1998). The soluble hAAG proteins tagged with hexahistidine (His_6) tag were purified to apparent homogeneity using three chromatographic steps: His-Trap Sepharose gel affinity column (Amersham Biosciences), and His_6 tag removal with PreScission Protease (Pharmacia) treatment overnight at 16^{o}C, His-Trap Sepharose gel affinity purification, and finally HiTrap sepharose cation exchange (Amersham Biosciences) and Superdex-75 gel filtration (Amersham Pharmacia Biotech) in gel filtration buffer (20mM HEPES, pH 7.5, 100mM NaCl, 1mM DTT, 5mM EDTA, and 10% glycerol). The final purified hAAG proteins were stored in the gel filtration buffer and were greater than 95% pure as evidenced by SDS-PAGE analysis.

DNA glycosylase activity assays:

DNA glycosylase assays were performed at 37^{o}C in a buffer containing 20 mM Tris-HCl pH 7.8, 100 mM KCl, 5mM β- mercaptoethanol, 6 mM EDTA, 4 nM double stranded ^{32}P-labeled DNA oligonucleotides containing hAAG substrates and 400 nM purified hAAG. The oligos were cleaved at AP-sites with 30 min 0.1 N NaOH treatment at 70ºC. Reaction products were separated on a 20% urea denaturing gel, imaged with Molecular Dynamics PhosphorImager and quantified using Kodak ID 1.0 software.

For excision of 3MeA and 7MeG, tritiated calf thymus DNA was incubated with hAAG glycosylases in glycosylase buffer (20 mM Tris pH 7.6, 100 mM KCl, 5 mM EDTA, 1 mM EGTA, 5 mM β-mercaptoethanol and BSA to 500 nmol of total protein per reaction) for indicated amounts of time. The reaction was terminated by the addition of 0.1 volume of sodium acetate buffer and DNA was precipitated with ethanol. Bases released by DNA glycosylase were spotted onto Whatman 3MM paper and descending paper chromatography was performed for 18 hrs in 70% isopropanol, 20% water and 10% ammonium hydroxide. Radioactivity was counted with Beckman LS6000IC scintillation counter.

Gel mobility shift assays:

Protein-DNA binding assays were carried out in buffer containing 4 mM Tris-HCl pH 7.8, 6 mM Hepes-KOH pH 7.8, 20 mM KCl, 30 mM NaCl, 0.5 mM EDTA, 1 mM β-mercaptoethanol, 10 ng Salmon Sperm DNA, 10% glycerol, and 0.5 nM ^{32}P-labeled DNA oligonucleotides (oligos) containing known or putative hAAG substrates. Purified hAAGs were incubated in the buffer at 4ºC for 30 min and separated on a 5% non-

denaturing polyacrylamide gel (PAGE). The gel was run in 0.5x TBE buffer at 130 V and 4ºC for 210 min, vacuum dried onto 3 MM Whatman paper, imaged with Molecular Dynamics PhosphorImager and quantified using Kodak ID 1.0 software.

Klapacz et al., Supplementary Figure 1

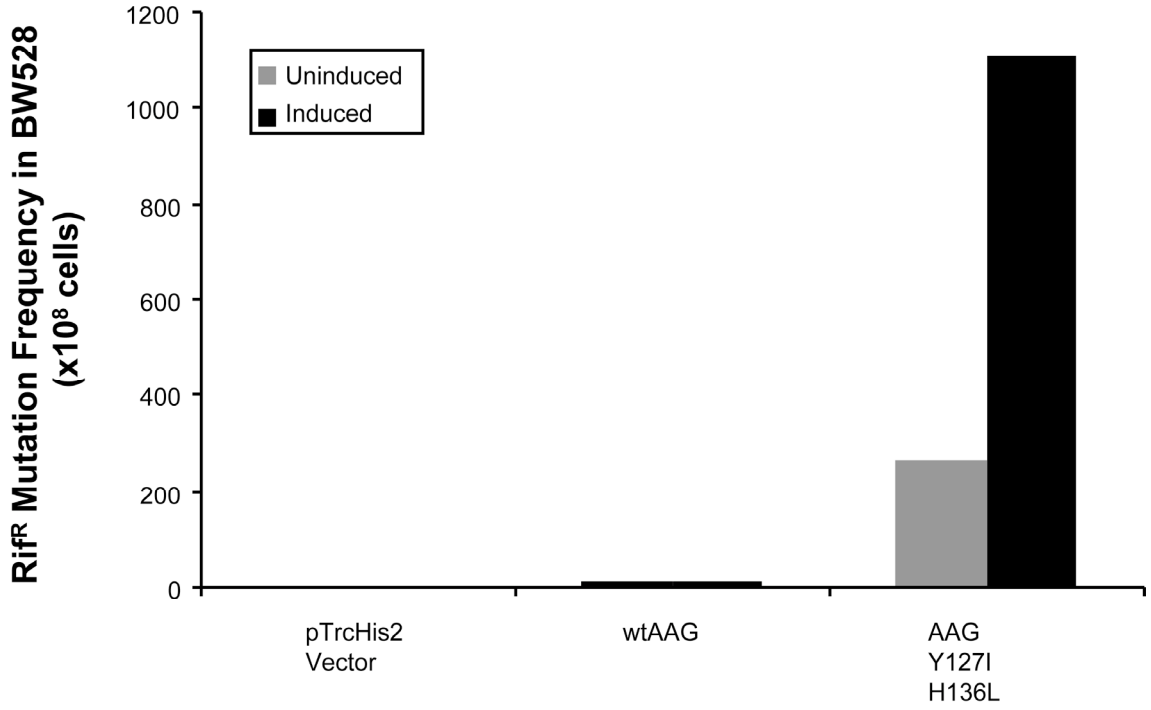

Klapacz et al., Supplementary Figure 2

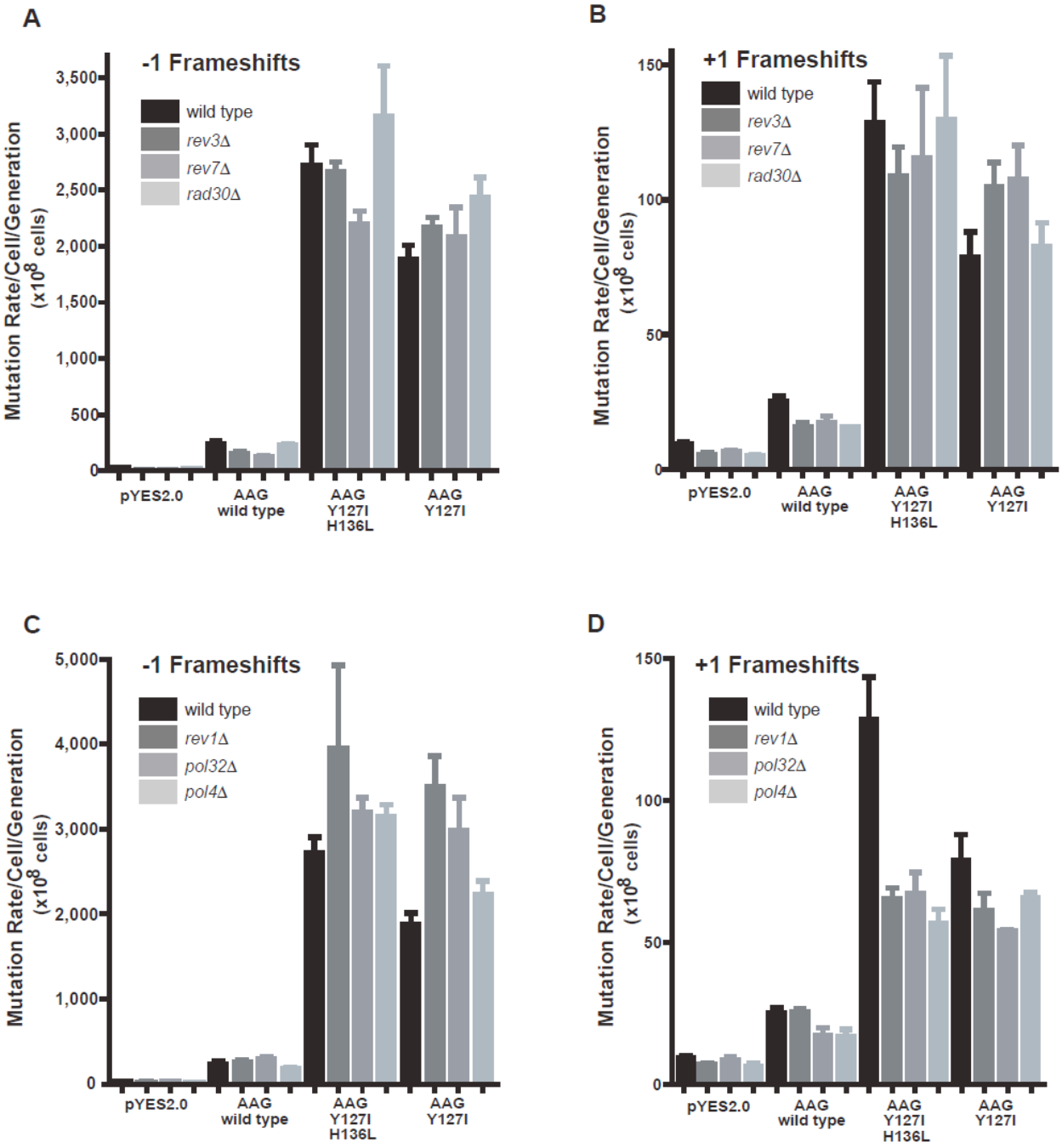

Klapacz et al., Supplementary Figure 3

A

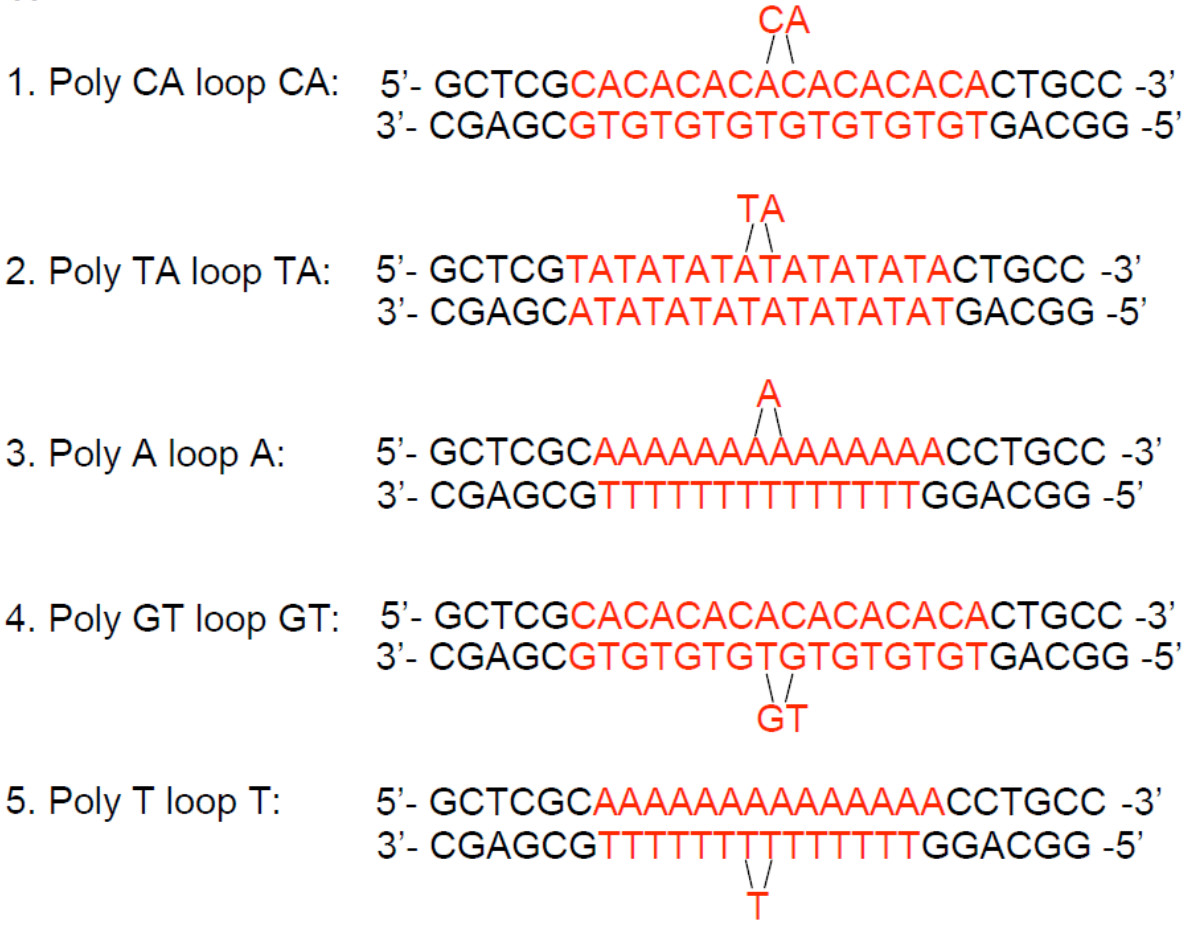

B

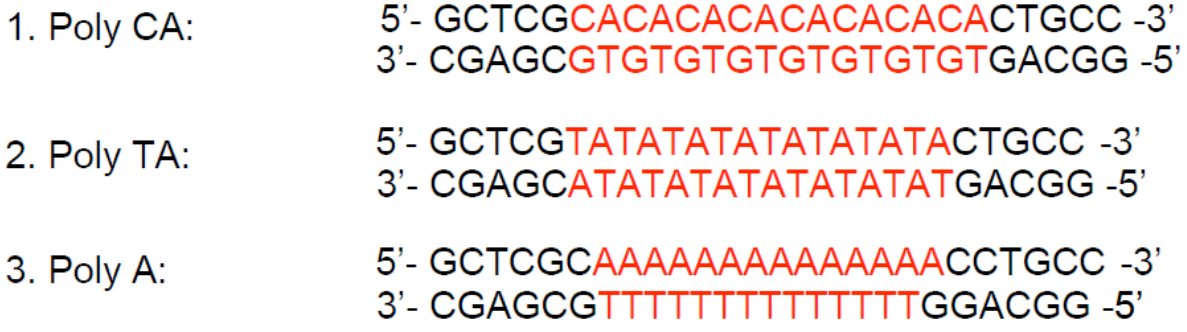

Klapacz et al., Supplementary Figure 4

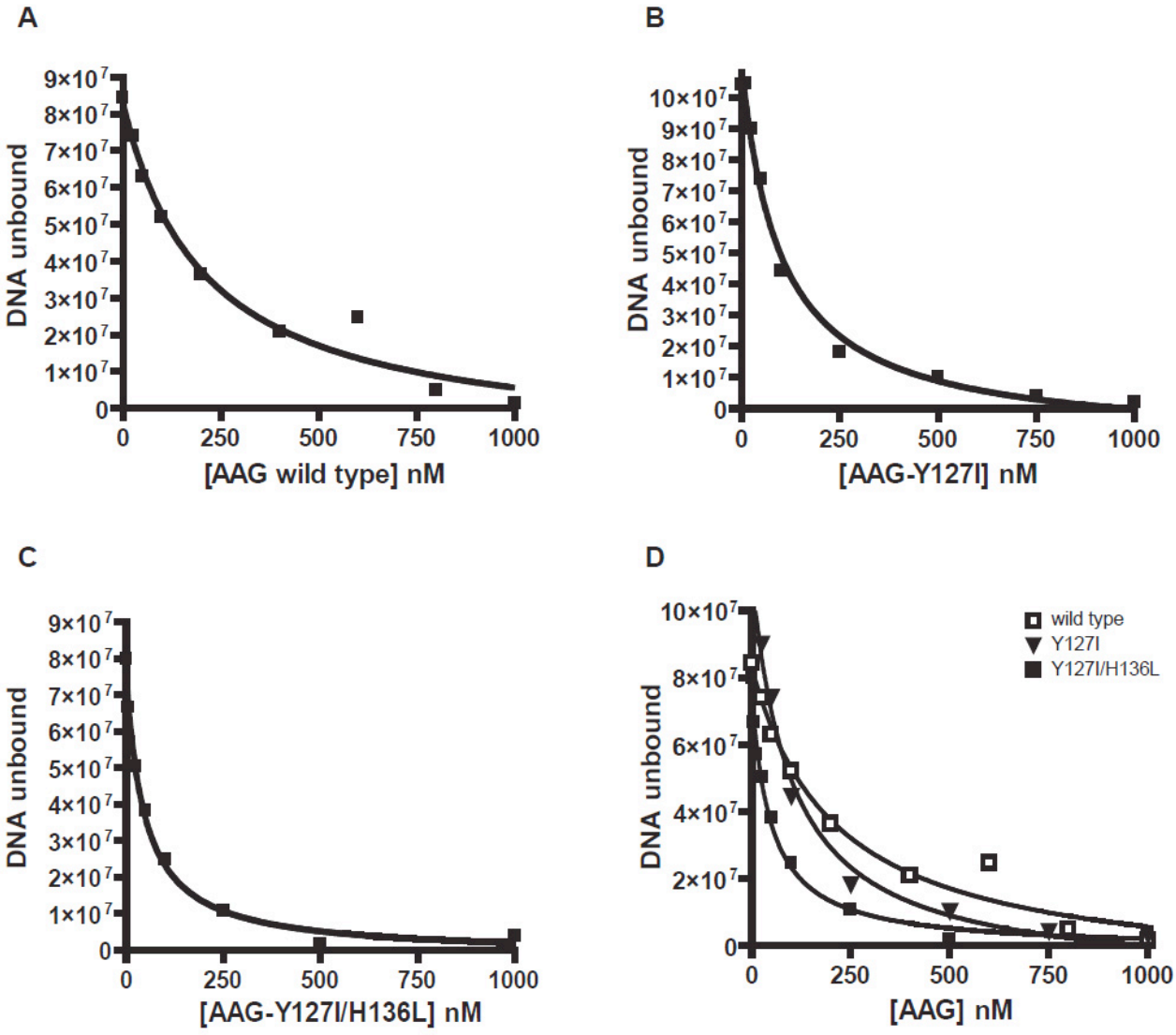

Supplemental Figure Legends

Figure S1:

Rifampicin resistance of *E. coli* BW528 expressing hAAG proteins.

hAAG cDNAs were expressed from the pTrcHis vector in *E. coli* cells by adding IPTG (isopropyl β-D-thiogalactoside) to the final concentration of 1mM. After each selection round, Rif^R colonies were picked, plasmids were isolated and the individual clones were re-transformed and re-assessed for their ability to confer an increased Rif^R frequency. A double hAAG mutant with the substitutions Y127I and H136L was thus isolated. pTricHis2 plasmids with wild type and AAG-Y127I/H136L cDNAs were introduced into BW528 cells and expressed overnight. IPTG was added to the final concentration of 1mM where indicated. Rif^R cells were selected on LB plates with 150μg/ml Rif. Mutation frequency was calculated as total number of mutants counted per 10^8 cells plated. This cDNA was then re-cloned into eukaryotic expression vectors alongside its respective single mutants and wild type *AAG* cDNAs.

Figure S2:

Effects of inactivation of DNA polymerases on hAAG-induced frameshift rates.

The mutation rates observed in wild-type yeast are represented in black and those observed in yeast deletion backgrounds are represented in different shades of gray. Mutation rates in wild-type, *rev3Δ*, *rev7Δ* and *rad30Δ* backgrounds for hAAG-induced (A) -1 frameshifts and (B) +1 frameshifts. Similarly, mutation rates in wild-type, *rev1Δ*, *pol32Δ* and *pol4Δ* backgrounds for hAAG-induced (C) -1 frameshifts and (D) +1

frameshifts. The n values for the most bars in all graphs are equal to 3 (n=3), except for bars with their respective n value is mentioned in parenthesis above.

Figure S3:

Sequences of polynucleotide DNA substrates that either, (A) contain base pair-loops; or (B) that do not contain base pair-loops.

Figure S4:

Quantitative binding of hAAG proteins to poly-A-loop-A containing DNA.
Plots showing the calculation of binding affinity (Kd) values presented in Table 2 for the binding of (A) wild type hAAG, (B) hAAG-Y127I, (C) hAAG-Y127I/H136L and (D) all three proteins combined in one plot to poly-A-loop-A containing oligonucleotides. The experiments were performed by gel shift assays, using different concentrations of hAAG proteins (0-1000 nM) and ^{32}P-labeled poly-A-loop-A oligonucleotide substrate. The Kd values were calculated as indicated in Materials and Methods section by fitting the data to the equation (3).

Supplemental Tables

Table S1. List of expression vectors used in the study.

Plasmid	**Purpose**	**Source**
pTrcHis	*E. coli* hAAG-mutant library creation and selection of Rif^R-producing clones	Invitrogen
pET19b-PPS	*E. coli* hAAG protein purification	Lau et al., 1998; Lau et al. 2000
pYES2.0	*S. cerevisiae* expression of 3MeA DNA glycosylases	Invitrogen; Glassner et al. 1998
pCAGGS	High-expression eukaryotic vector for hAAG protein expression in K562 cells	Niwa et al., 1991
pMACS-KkII	Co-transfection with pCAGGS and positive K562 clone isolation	Miltenyi Biotech

Table S2. List of strains used in the study.

Strain	Genotype	Reference
S. cerevisiae		
E133	*MATα ade5-1 his7-2 leu2-3,112 trp-289 ura3-52 lys2::InsE-A12*	(Tran et al., 1997)
E134	*MATα ade5-1 his7-2 leu2-3,112 trp-289 ura3-5 lys2::InsE-A14*	(Tran et al., 1997)
E133*apn1Δ*	E133 *apn1-Δ1::HIS3*	(Rusyn et al., 2007)
E134*apn1Δ*	E134 *apn1-Δ1::HIS3*	(Rusyn et al., 2007)
E133*rev1Δ*	E133 *rev1-Δ::kanMX4*	This study
E133*rev3Δ*	E133 *rev3-Δ::HIS3*	(Rusyn et al., 2007)
E133*rev7Δ*	E133 *rev7-Δ::kanMX4*	This study
E134*rev1Δ*	E134 *rev1-Δ::kanMX4*	This study
E134*rev3Δ*	E134 *rev3-Δ::kanMX4*	This study
E134*rev7Δ*	E134 *rev7-Δ::HIS3*	(Rusyn et al., 2007)
E133*rad30Δ*	E133 *rad30Δ::kanMX4*	This study
E134*rad30Δ*	E134 *rad30-Δ::kanMX4*	This study
E133*pol32Δ*	E133 *pol32-Δ::kanMX4*	This study
E134*pol32Δ*	E134 *pol32-Δ::kanMX4*	This study
E133*pol4Δ*	E133 *pol4-Δ::kanMX4*	This study
E134*pol4Δ*	E134 *pol4-Δ::kanMX4*	This study
E133*msh2Δ*	E133 *msh2-Δ::kanMX4*	This study
E133*msh6Δ*	E133 *msh6-Δ::kanMX4*	This study
E133*msh3Δ*	E133 *msh3-Δ::kanMX4*	This study
E134*msh6Δ*	E134 *msh6-Δ::kanMX4*	This study
E134*msh3Δ*	E134 *msh3-Δ::kanMX4*	This study
BGY111	*MATα his3 leu2-Δ trp-289$_{\alpha}$ ura3-52*	(Glassner et al., 1998b)
BGY148	BGY111 *mag1Δ2::LEU2*	(Glassner et al., 1998b)
E. coli		
AB1157	*F⁻ thr-1 leu-6 proA2 thi-1 argE lacY1 galK ara-14 xyl-5 mtl-1 tsx-33 strA sup-37*	Lab stock
BW528	*AB1157* Δ*xth-pncA nfo-1*::Kan	Lab stock
BL21(DE3)	*F⁻ ompT hsdS*(rB⁻ mB⁻) *dcm*$^{+}$ Tet^{r} *gal* λ(DE3) *endA* Hte	Lab stock
XL10 Gold	Tet^{r} Δ(*mcrA*)*183* Δ(*mcrCB-hsdSMR-mrr*)*173 endA1 supE44 thi-1 recA1 gyrA96 relA1 lac* F′ *proAB lacI*qZΔ*M15* Tn*10* Cam^{r}	Stratagene

Table S3. List of oligonucleotides used in the study. For site directed mutagenesis, mutated codons are shown bold and underlined.

Primers	**Sequence (5'-3')**
pCAGGS cloning	Forward: AGTCCTCGAGACCATGGTCACCCCCGCTTTGCAG
	Reverse: AGTCCTCGAGTCAGGCCTGTGTGTCCTGCTC.
hAAG PCR	Forward: GGAAGGAAATGGGCGGGGAGGGCC
	Reverse: CGCAAGCCCCGTCCCCCTGGCTGGAG
hAAG RT-PCR	Forward: CCCATACCGCAGCATCTATT
	Reverse: CGGAGTTCTGTGCCATTAGG
hAAG mutant Y127I	Forward: CGCATCGTGGAGACTGAGGCA**ATC**CTGGGGCCAGAGG
	Reverse: CCTCTGGCCCCAG**GAT**TGCCTCAGTCTCCACGATGCG
hAAG mutant H136L	Forward: GATGAAGCCGCC**CTG**TCAAGGGGTGGCCG
	Reverse: CGGCCACCCCTTGA**CAG**GGCGGCTTCATC
hAAG mutant E125A (with Y127I mutants)	Forward: CGCATCGTGGAGACC**GCC**GCA**ATC**CTGGGGCCAG
	Reverse: CTGGCCCCAG**GAT**TGC**GGC**GGTCTCCACGATGCG
hAAG mutant E125A (with wild type)	Forward: CGCATCGTGGAGACT**GCC**GCATACCTGGGGCCAG
	Reverse: CTGGCCCCAGGTATGC**GGC**AGTCTCCACGATGCG